

# Design and Development of Mathematical and Thermal Load Modelling for Induction Heating Systems

Pradeep Vishnuram<sup>1</sup>, A. Muni Sankar<sup>2</sup>, Anitha D<sup>3\*</sup>, J. Ganesh Prasad Reddy<sup>4</sup>, Mohit Bajaj<sup>5,6,7</sup>

<sup>1,3</sup>Department of Electrical and Electronics Engineering, SRM Institute of Science and Technology, Kattankulathur, Chennai-603203, Tamilnadu, India; Email: <sup>1</sup>pradeep.kannan03@gmail.com, <sup>3</sup>anithad1@srmist.edu.in

<sup>2</sup>Department of EEE, Sree Rama Engineering College, Tirupati, A.P, India; Email: munisankar.eee@gmail.com

<sup>4</sup>Department of EEE, AM Reddy Memorial College of Engineering and Technology, Narasaraopet-522601 Palnadu, A.P, India; Email: jgpreddy@gmail.com

<sup>5</sup>Department of Electrical Engineering, Graphic Era (Deemed to be University), Dehradun-248002, India; Email: thebestbajaj@gmail.com

<sup>6</sup>Hourani Center for Applied Scientific Research, Al-Ahliyya Amman University, Amman, Jordan

<sup>7</sup>Graphic Era Hill University, Dehradun, 248002, India

\*Correspondence: anithad1@srmist.edu.in

**ABSTRACT-** Complex systems can be modelled and their performance can be anticipated with the help of current computers and software tools that are applicable in real-world situations. The IH system is capable of being modelled and put through analysis in two distinct domains. The modelling is compatible with the research and applications in their entirety, including the particular control circuits and converter systems under consideration. The use of electrical modelling makes it possible to analyse the features of the IH load and to examine the variations in the parameters in order to determine the impact of load variations. In order to gain an understanding of the load's flow and thermal distribution, thermal modelling is a crucial component of this study. For the purpose of analysing the performance of the coil in terms of flux and temperature from its comparable model, the COMSOL Multiphysics software that is utilised is utilised.

**Keywords:** Induction heating, load modelling, COMSOL simulation, power converters.

## ARTICLE INFORMATION

**Author(s):** Pradeep Vishnuram, A. Muni Sankar, Anitha D, J. Ganesh Prasad Reddy, Mohit Bajaj;

**Received:** 02/02/2024; **Accepted:** 18/04/2024; **Published:** 30/04/2024;

**E- ISSN:** 2347-470X;

**Paper Id:** IJEER24040A;

**Citation:** 10.37391/IJEER.120210

**Webpage-link:**

<https://ijeer.forexjournal.co.in/archive/volume-12/ijeer-120210.html>



**Publisher's Note:** FOREX Publication stays neutral with regard to jurisdictional claims in Published maps and institutional affiliations.

## 1. INTRODUCTION

Natural gas, a fossil fuel that contributes to impending global warming by making heating, cooking, and electricity generation more difficult, is the most used fuel source for these applications [1]. On the other side, IH is responsible for conserving clean energy while maintaining higher efficiency [2], [3]. Compared to more traditional heating technologies like resistive heating, flames heating, or welding equipment, it is more effective and efficient, making it a preferable option for industrial applications [4], [5]. Most notably, IH's inbuilt safety and convection methods are particularly suitable for various medical applications [6], [7]. IH's portability and "plug and play" functionality are particularly in-demand features in residential settings [8].

Single-switch resonant inverters are the type of inverter that is recommended for use in an IH system when the power demand for the system is less than 2 kW. A single-switch concurrent resonant AC-AC converter was utilised by Shenkman et al. for their applications in the field of information technology [9]. Through the utilisation of a single switch that was coupled in series with the supply voltage, this converter was able to generate high-frequency alternate current (HFAC). The utilisation of an LC filter resulted in an improvement to the power factor of the particular source. The variable frequency power regulation method, on the other hand, resulted in increasing switching losses. The solution to this problem was to implement a control strategy that utilised a fixed frequency and multi-cycle modulation [10]. Through the use of two input semiconductor SiC linking gate field-effect transistors, the conversion of 50 Hz AC voltage to HFAC was accomplished. For the purpose of reducing switching losses, both switches were operating in a mode that is known as soft switching [11].

The half-bridge (HB) series resonant inverter (SRI) is the preferred choice for applications with power ratings between 2000 W and 4000 W. Ahmed et al. [12] designed a boost HB inverter that featured LC branches on the supply side. This resulted in increased efficiency by lowering the amount of DC and high-frequency components that were present in the system. Furthermore, the time constant of the system is lengthened as new LC networks are incorporated into the system. Forest et al. [13] developed an induction heating system using a multi-

winding induction coil to address the issue of various load shapes. The system utilised square and rectangular coils to allow power control by adjusting the inverter's switching frequency. An approach to control was developed by Lucia et. al., [14] in order to estimate load parameters in the presence of dynamic variations. The inverter switches were controlled by a field-programmable gate array (FPGA) controller, and the switching frequency ranged from 20 to 100 kHz when they were in operation. We measured the inductance and resistance of the load at several switching frequencies. To supply power to several loads, Lucia et al. created an induction cooking system that is based on multiple coils [15]. The PDM approach, which involved the fewest possible switching losses, was used to regulate the output power. To achieve higher productivity levels when dealing with light loads, Lucia et al. created a multi-inverter that functioned in an irregular conduction mode [16].

An AC-AC matrix converter for cooking applications is proposed in [17]. An HB bidirectional switch was used to convert commercial AC supply to HFAC supply and many loads were connected in parallel through a single switch. Sarnago et. al., used a boost HB inverter, in which the output voltage was boosted by reducing the current for the same power rating [18]. An adaptive load control for induction cooking applications is proposed using FPGA controller [19]. The load parameters' inductance and resistance were evaluated using sigma-delta ADCs and a discrete-time Fourier computational technique. Sarnago et. al., used reverse-blocking IGBT for an HB inverter with an anti-parallel diode. This switch allows the circulating current to the diode resulting in minimum switching losses. The system provides higher efficiency (98.4%) at rated load conditions. A dual-mode resonant inverter is proposed in [10]. In this circuit, the system's efficiency was improved at low-medium frequency conditions by connecting an additional capacitor through the mechanical relay. The inverter was capable of operating in both Class-D and Class-E modes. However, the mechanical relay requires a separate control mechanism. Two partially-coupled coils with two HB inverter is developed in [20]. The self and mutual coupling inductance were measured using the finite element calculus method.

An online power measurement to estimate the load parameters concerning heat rate and efficiency is developed in [21]. Due to dynamic variations, the online estimated parameters were subjected to sudden variations of voltage and current, resulting in the non-safer operation of the inverter. A multi-load IH system with switched capacitor was developed by [22]. The output power control was performed using AVC PWM control resulting in ZVS operation for a wide range of load variations. The power regulation was found to be 8% larger than the traditional control, and the THD of source voltage was maintained within 5%. Mishima et. al. used a twin HB inverter. The output power was controlled by changing the phase angle between two adjacent legs of the inverter [23]. Jimenez et. al., used an IH emulator to detect the switching characteristics and to measure the efficiency [21].

Sanz Serrano et. al. studied the coupling effect and the temperature distribution on the coil using FEM software [26]. A power factor correction rectifier for multi-load applications

is proposed in [24]. The proposed circuit not only corrects the power factor but also boosts the input voltage. The inverter was operated in both continuous conduction (CC) and discontinuous conduction (DCC) modes, and it was observed that the efficiency was better in CC mode. The developed split output HB (SOHB) AC-AC converter. Each SOHB inverter was built to handle a single load, and inverters were arranged to handle multiple loads in matrix form [25].

Existing literature indicates a clear effort to develop a load model for the IH system. This study aims to enhance the electrical and thermal modelling of the IH load. This study is conducive for the kindle researchers interested in working on the IH application. The mathematical model of the IH load is electrically modelled, and the parametric variation studies various operating conditions. Also, the flux distribution and temperature variation are studied using COMSOL multi-physics software.

## 2. MATHEMATICAL ANALYSIS OF THE INDUCTION HEATING LOAD

A work coil and a vessel pan comprise an IH system (workpiece). There is an electrical separation between the vessel pan and the work coil. The IH system's equivalent circuit resembles the transformer model in which the work coil is primary, and the workpiece is secondary. When the HFAC supply is applied to the primary side, the eddy current is generated on the material to be heated by electromagnetic induction. The equivalent circuit of the work coil and workpiece is shown in *fig. 1*.

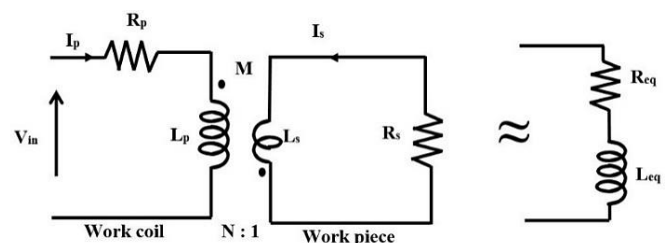


**Figure 1.** Equivalent circuit of work coil and workpiece

Let  $L_p$  be the self-inductance of the work coil and work coil resistance be  $R_p$ . Let's say that the coil's mutual inductance is denoted by the letter  $M$ . Both the resistance and the inductance of the work piece are denoted by the symbols  $R_s$  and  $L_s$ , respectively. The current moving through the work coil is denoted by  $I_p$ , while  $I_s$  denotes the load. KVL was applied to the circuit indicated in *fig. 1*, which was an equivalent circuit.

$$(R_p + j\omega_s L_p)I_p - j\omega_s M I_s = V_{in} \quad (1)$$

$$(R_s + j\omega_s L_s)I_s - j\omega_s I_p M = 0 \quad (2)$$

The angular switching frequency ( $\omega_s$ ) is

$$\omega_s = 2\pi f_s \quad (3)$$

The current flowing through the load is

$$I_s = \frac{j\omega_s M I_p}{R_s + j\omega_s L_s} \quad (4)$$

Letting eq. (4) in eq. (1) and (2)

$$V_{in} = R_p + \frac{\omega_s^2 M^2 R_s}{R_s^2 + \omega_s^2 L_s^2} + j\omega_s \left[ L_p + \frac{\omega_s^2 M^2 L_s}{R_s^2 + \omega_s^2 L_s^2} \right] \quad (5)$$

$$R_{eq} = R_p + \frac{\omega_s^2 M^2 R_s}{R_s^2 + \omega_s^2 L_s^2} \quad (6)$$

$$L_{eq} = L_p + \frac{\omega_s^2 M^2 L_s}{R_s^2 + \omega_s^2 L_s^2} \quad (7)$$

From eq. (6) and (7), the mutual inductance (M) is

$$M^2 = \frac{(R_{eq} - R_p)(R_s^2 + \omega_s^2 L_s^2)}{\omega_s^2 R_s} \quad (8)$$

The resonant frequency  $f_r$  is

$$f_r = \frac{1}{2\pi\sqrt{L_{eq} C_r}} \quad (9)$$

Where  $C_r$  is a resonant capacitor

The coil's quality factor is

$$Q = \frac{2\pi f_r L_{eq}}{R_{eq}} \quad (10)$$

Eqns. 6 and 7 are used to compute the equivalent resistance and inductance of the IH load.

### 3. ANALYSIS OF IH LOAD WITH HIGH-FREQUENCY AC SUPPLY

When resonant converters are utilized in IH-based applications, frequency management is a significant factor to consider. Adding a resonant capacitor  $C_r$  to an existing IH resonance tank creates an RLC resonance tank by matching the resistance and inductance of the existing system. The load is heated via the production of high-frequency alternating current (HFAC) sinusoidal current under resonance conditions by the capacitor. The equivalent circuit of an IH load with  $C_r$  is depicted in figure 2.

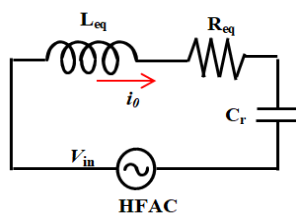


**Figure 2.** Equivalent circuit IH load with the resonant capacitor

To study the performance of the IH system, the design specifications considered are  $V_{in} = 50$  V,  $f_s = 20$  kHz,  $P_0 = 500$  W,  $R_{eq} = 3.5$   $\Omega$ ,  $L_{eq} = 0.05$  mH and  $C_r = 1.3$   $\mu$ F. Fig. 3 depicts the change in power concerning the switching frequency. It is inferred that the maximum output power at the resonance frequency decreases as the switching frequency increases or decreases. Hence, the output power can vary by increasing or decreasing the switching frequency. When it is operated above the resonance condition, the current is more inductive and capacitive below the resonance operation.

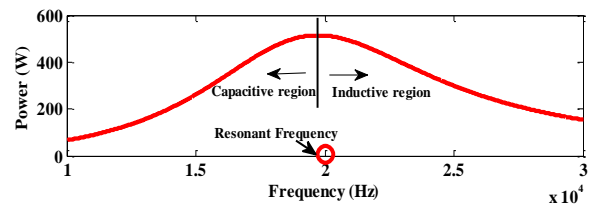


**Figure 3.** Change in power concerning frequency

In the variable frequency operation, it is always necessary to understand the variation in load parameters. Thus, there is a need to estimate the resistance and inductance concerning switching frequency variations. The skin depth ( $\delta$ ) and equivalent resistance of the load is

$$\delta = \sqrt{\frac{\rho}{\pi\mu f_s}} \quad (13)$$

$$R_{eq} = \frac{\rho l}{A} \quad (14)$$

Where  $\rho$  is the resistivity,  $\mu$  is the permeability,  $f_s$  is the switching frequency, 'l' represents the length of the material, 'A' denotes the area of the cross-section. The variation of the resistance concerning the frequency is shown in fig. 4. It is observed that, for an increase in frequency, the skin depth of the material decreases; thereby, the resistance increases. Similarly, the change in inductance concerning increased switching frequency is shown in fig. 5. As the switching frequency increases, the inductance decreases. From the results, it is inferred that as variable frequency control is deployed to control the output power, the resistance and inductance values change dynamically. Therefore, variable frequency controllers should be developed only after considering the resistance and inductance values. The resistance of the coil can be reduced by increasing the thickness or resistivity of the coil.

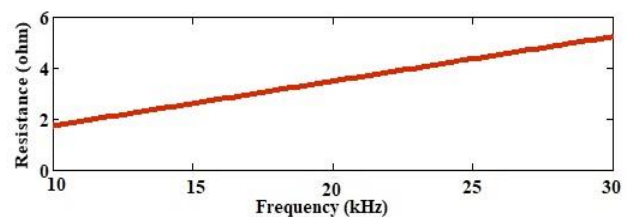


**Figure 4.** Change in resistance concerning frequency

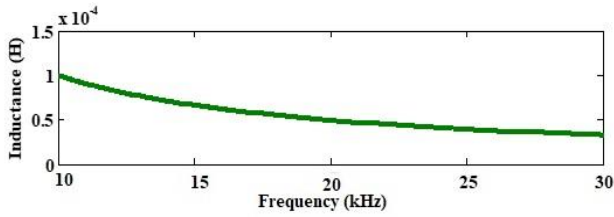


**Figure 5.** Change in inductance concerning frequency

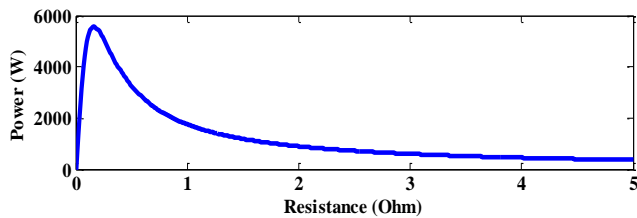


**Figure 6.** Change in power concerning resistance

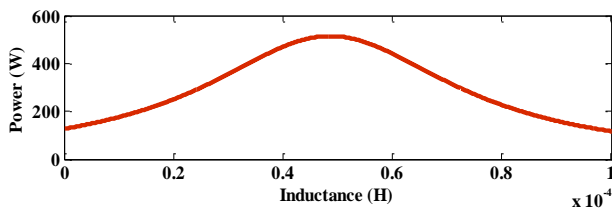


**Figure 7.** Change in power concerning inductance

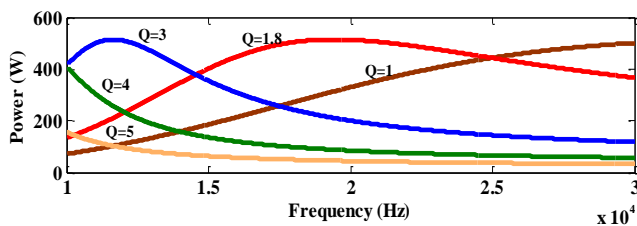


**Figure 8.** Change in power concerning inductance for various quality factors

For a fixed frequency of 20 kHz, the change in power concerning resistance is shown in *fig. 6* and *fig. 7* depicts the change in power concerning inductance. The resonant frequency of the coil varies concerning the quality factor, as shown in *fig. 8*. From responses, it is inferred that the power varies for the variations in the quality factor of the coil. Hence, an appropriate controller is required to regulate the output power per the load requirement. *Table 1* outlines the parameters utilised to evaluate the analytical solution of the FEM simulation model.

**Table 1: Parameters to determine the analytical solution**

Variables	Values	Variables	Values
R	0.025 m	$f_s$	20000 Hz
b	0.018 m	$\sigma$	$6 \times 10^7$ [S/m]
l	0.016 m	$\rho_c$	8700 [kg/m <sup>3</sup> ]
N	21	$C_p$	387 [J/(kg*K)]
$L_s$	0.002 mH	$T_\infty$	273 K
$R_{eq}$	0.3 $\Omega$	$\epsilon_r$	0.5

The finite element analysis tool is essential for analysing the IH load model with the specified geometry. The 2-D model of the induction heating load is shown in *fig. 9*. Iron coil is considered as the workpiece, and the copper coil is used as the work coil. The whole arrangement is placed in the air medium. The 3-D model of IH load is shown in *fig. 10*. Its corresponding magnetic distribution is shown in *fig. 11*. It is inferred that the flux produced in the work coil is linked with the workpiece, due to which eddy current flows on the surface of the iron rod. The temperature distribution in the IH load is illustrated in *fig. 12*. It is evident that when the coil is subjected to HFAC, the workpiece gets heated and the temperature increases.

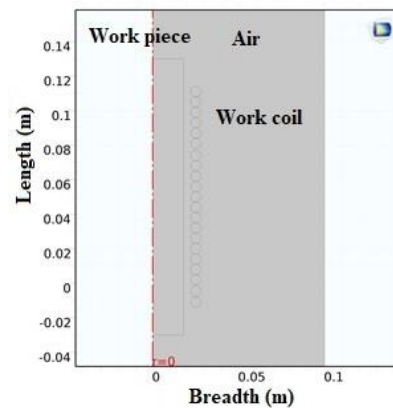


**Figure 9.** 2-D Model of IH load

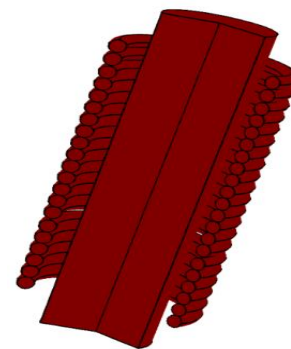


**Figure 10.** 3-D Model of IH load

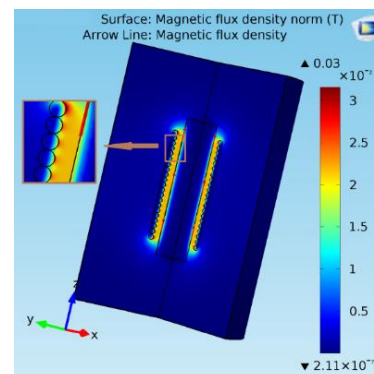


**Figure 11.** Magnetic flux distribution in IH load



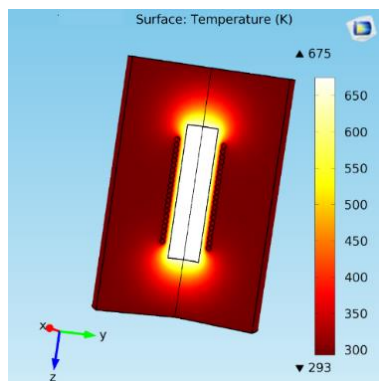


**Figure 12.** Temperature distribution in IH load

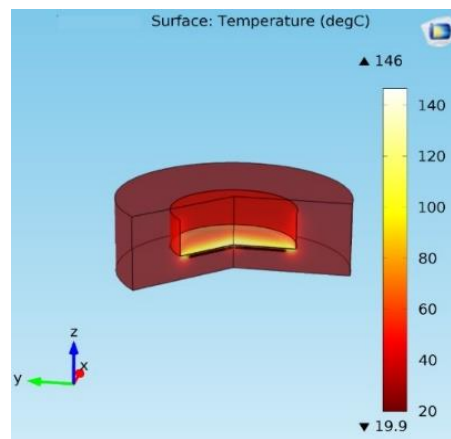


**Figure 16.** Temperature distribution in induction cooking load

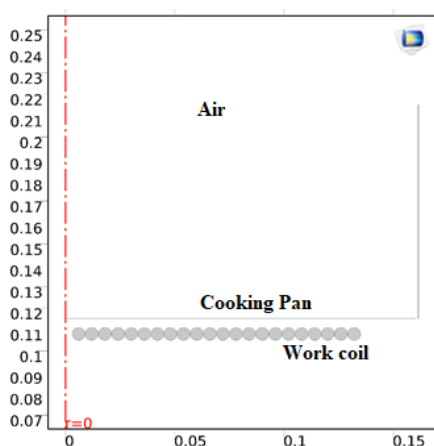


**Figure 13.** 2-D geometric model of induction cooking load

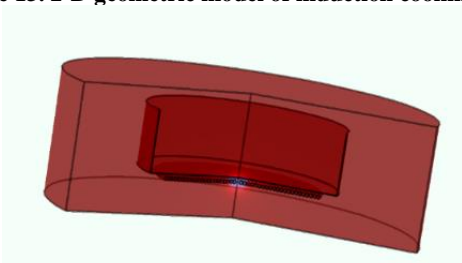


**Figure 14.** 3-D Model of induction cooking load

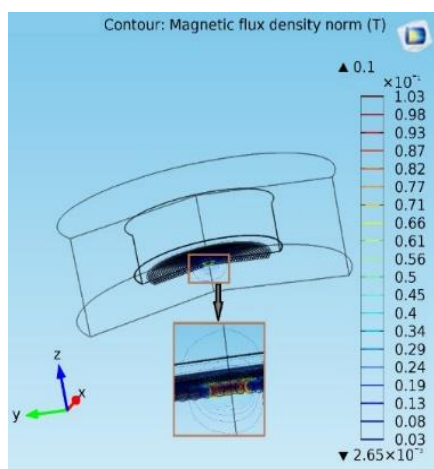


**Figure 15.** Magnetic flux distribution in induction cooking load

The 2-D geometric model of the cooking load is illustrated in *fig. 13*. The 3-D model of induction cooking load is shown in *fig. 14*. When the cooking coil is subjected to HFAC, more magnetic flux is produced in the centre of the coil as shown in *fig. 15*. The distribution of flux is more at the middle of the coil which results in high temperature at the centre as shown in *fig. 18*. Also, the air gap between coil and load is less in centre of the coil, which results in less leakage flux when compared to the trailing edge. The nature of the flux density and temperature rise for various time instances are studied for induction cooking load.

#### 4. CONCLUSION

This work discusses detailed modelling and simulation of the IH load. MATLAB and COMSOL Multi-Physics Software is found to be the most potent and predominantly used simulation tool by researchers and engineers. The importance of modelling IH load and its variation of the output parameters concerning the various set constraints is realized in this section. A geometric model of the IH load is created and simulated using Finite Element Method (FEM) software. Furthermore, the temperature distribution and magnetic flux density are analysed using COMSOL Multiphysics software. The concluding remarks of this work are

- A typical mathematical model of IH load is derived from calculating the equivalent resistance and inductance.
- When the frequency is varied, the load resistance, inductance and power vary. Thus, an excellent controller is required to regulate the output power.

COMSOL Multiphysics software gives the best response in knowing the work piece's temperature and flux distribution.

#### AUTHOR CONTRIBUTIONS

All authors contributed to the study, conception and design. Material preparation, data collection and analysis were performed by AD, PV and MB. The first draft of the manuscript was written by JGPR and AMS and all authors commented on previous versions of the manuscript. All authors read and approved the final manuscript.

## 5. REFERENCES

- [1] H. Bai, X. Wang, and F. Blaabjerg, "Passivity Enhancement in Renewable Energy Source Based Power Plant With Paralleled Grid-Connected VSIs," *IEEE Trans. Ind. Appl.*, vol. 53, no. 4, pp. 3793–3802, Jul. 2017, doi: 10.1109/TIA.2017.2685363.
- [2] V. T. Kilic, E. Unal, and H. Volkan Demir, "High-efficiency flow-through induction heating," *IET Power Electron.*, vol. 13, no. 10, pp. 2119–2126, Aug. 2020, doi: 10.1049/iet-pel.2019.1609.
- [3] P. Vishnuram, G. Ramachandiran, T. Sudhakar Babu, and B. Nastasi, "Induction Heating in Domestic Cooking and Industrial Melting Applications: A Systematic Review on Modelling, Converter Topologies and Control Schemes," *Energies*, vol. 14, no. 20, p. 6634, Oct. 2021, doi: 10.3390/en14206634.
- [4] P. Vishnuram, G. Ramachandiran, S. Ramasamy, and S. Dayalan, "A comprehensive overview of power converter topologies for induction heating applications," *Int. Trans. Electr. Energy Syst.*, vol. 30, no. 10, Oct. 2020, doi: 10.1002/2050-7038.12554.
- [5] B. Nagarajan, R. R. Sathi, and P. Vishnuram, "Power Tracking Control of Domestic Induction Heating System using Pulse Density Modulation Scheme with the Fuzzy Logic Controller," *J. Electr. Eng. Technol.*, vol. 9, no. 6, pp. 1978–1987, Nov. 2014, doi: 10.5370/JEET.2014.9.6.1978.
- [6] P. Vishnuram and G. Ramachandiran, "Capacitor-less induction heating system with self-resonant bifilar coil," *Int. J. Circuit Theory Appl.*, vol. 48, no. 9, pp. 1411–1425, Sep. 2020, doi: 10.1002/cta.2830.
- [7] P. Vishnuram and S. Ramasamy, "Fuzzy Logic-Based Pulse Density Modulation Scheme for Mitigating Uncertainties in AC–AC Resonant Converter Aided Induction Heating System," *J. Circuits, Syst. Comput.*, vol. 28, no. 02, p. 1950030, Feb. 2019, doi: 10.1142/S0218126619500300.
- [8] J. Villa, D. Navarro, A. Dominguez, J. I. Artigas, and L. A. Barragan, "Vessel Recognition in Induction Heating Appliances—A Deep-Learning Approach," *IEEE Access*, vol. 9, pp. 16053–16061, 2021, doi: 10.1109/ACCESS.2021.3052864.
- [9] S. S. H. K. B. J. Reddy, R. Dash and V. Subburaj, "Dual-Topology Cross-Coupled Configuration of Switched Capacitor Converter for Wide Range of Application," 2022 IEEE 21st Mediterranean Electrotechnical Conference (MELECON), Palermo, Italy, 2022, pp. 796-800, doi: 10.1109/MELECON53508.2022.9843051.
- [10] H. Samago, Ó. Lucia, A. Mediano, and J. M. Burdío, "Class-D/DE Dual-Mode-Operation Resonant Converter for Improved-Efficiency Domestic Induction Heating System," *IEEE Trans. Power Electron.*, vol. 28, no. 3, pp. 1274–1285, Mar. 2013, doi: 10.1109/TPEL.2012.2206405.
- [11] B. NAGARAJAN, R. R. SATHI, and P. VISHNURAM, "Fuzzy logic based voltage control scheme for improvement in dynamic response of the class D inverter based high frequency induction heating system," *TURKISH J. Electr. Eng. Comput. Sci.*, vol. 24, pp. 2556–2574, 2016, doi: 10.3906/elk-1403-57.
- [12] N. A. Ahmed and M. Nakaoka, "Boost-half-bridge edge resonant soft switching PWM high-frequency inverter for consumer induction heating appliances," *IEE Proc. - Electr. Power Appl.*, vol. 153, no. 6, p. 932, 2006, doi: 10.1049/ip-epa:20060086.
- [13] Kumar, Busireddy Hemanth, Makarand Mohankumar Lokhande, Karasani Raghavendra Reddy, and Vijay Bhanuji Borghate. "An improved space vector pulse width modulation for nine-level asymmetric cascaded H-bridge three-phase inverter." *Arabian Journal for Science and Engineering*. 2019, 44: 2453-2465.
- [14] O. Lucia, J. M. Burdío, I. Millan, J. Acero, and D. Puyal, "Load-Adaptive Control Algorithm of Half-Bridge Series Resonant Inverter for Domestic Induction Heating," *IEEE Trans. Ind. Electron.*, vol. 56, no. 8, pp. 3106–3116, Aug. 2009, doi: 10.1109/TIE.2009.2022516.
- [15] P. Vishnuram, G. Ramachandiran, and S. Ramasamy, "A Novel Power Control Technique for Series Resonant Inverter-Fed Induction Heating System with Fuzzy-Aided Digital Pulse Density Modulation Scheme," *Int. J. Fuzzy Syst.*, vol. 20, no. 4, pp. 1115–1129, Apr. 2018, doi: 10.1007/s40815-017-0408-9.
- [16] O. Lucia, J. M. Burdío, L. A. Barragan, C. Carretero, and J. Acero, "Series Resonant Multiinverter with Discontinuous-Mode Control for Improved Light-Load Operation," *IEEE Trans. Ind. Electron.*, vol. 58, no. 11, pp. 5163–5171, Nov. 2011, doi: 10.1109/TIE.2011.2126541.
- [17] Hemanth Kumar, B., and Makarand M. Lokhande. "Investigation of switching sequences on a generalized SVPWM algorithm for multilevel inverters." *Journal of Circuits, Systems and Computers*. 2019, 28, no. 02: 1950036.
- [18] H. Sarnago, A. Mediano, and Ó. Lucia, "High Efficiency AC–AC Power Electronic Converter Applied to Domestic Induction Heating," *IEEE Trans. Power Electron.*, vol. 27, no. 8, pp. 3676–3684, Aug. 2012, doi: 10.1109/TPEL.2012.2185067.
- [19] H. Sarnago, O. Lucia, A. Mediano, and J. M. Burdío, "Modulation Scheme for Improved Operation of an RB-IGBT-Based Resonant Inverter Applied to Domestic Induction Heating," *IEEE Trans. Ind. Electron.*, vol. 60, no. 5, pp. 2066–2073, May 2013, doi: 10.1109/TIE.2012.2207652.
- [20] Kasinath Jena, Dhananjay Kumar, B. Hemanth Kumar, K. Janardhan, Arvind R. Singh, Raj Naidoo, Ramesh C. Bansal, "A Single DC Source Generalized Switched Capacitors Multilevel Inverter with Minimal Component Count", *International Transactions on Electrical Energy Systems*, vol. 2023, Article ID 3945160, 12 pages, 2023. <https://doi.org/10.1155/2023/3945160>
- [21] O. Jimenez, O. Lucia, I. Urriza, L. A. Barragan, and D. Navarro, "Power Measurement for Resonant Power Converters Applied to Induction Heating Applications," *IEEE Trans. Power Electron.*, vol. 29, no. 12, pp. 6779–6788, Dec. 2014, doi: 10.1109/TPEL.2014.2304675.
- [22] B. Saha and R.-Y. Kim, "High Power Density Series Resonant Inverter Using an Auxiliary Switched Capacitor Cell for Induction Heating Applications," *IEEE Trans. Power Electron.*, vol. 29, no. 4, pp. 1909–1918, Apr. 2014, doi: 10.1109/TPEL.2013.2265984.
- [23] Kumar, Busireddy Hemanth.; and Vivekanandan Subburaj. Integration of RES with MPPT by SVPWM Scheme. *Intelligent Renewable Energy Systems*. 2022; 157-178. <https://doi.org/10.1002/9781119786306.ch6>
- [24] F. Sanz-Serrano, C. Sagues, and S. Llorente, "Power distribution in coupled multiple-coil inductors for induction heating appliances," in *2015 IEEE Industry Applications Society Annual Meeting*, IEEE, Oct. 2015, pp. 1–8. doi: 10.1109/IAS.2015.7356805.
- [25] H. Sarnago, P. Guillen, J. M. Burdío, and O. Lucia, "Multiple-Output ZVS Resonant Inverter Architecture for Flexible Induction Heating Appliances," *IEEE Access*, vol. 7, pp. 157046–157056, 2019, doi: 10.1109/ACCESS.2019.2950346.



© 2024 by Pradeep Vishnuram, A. Muni Sankar, Anitha D, J. Ganesh Prasad Reddy, Mohit Bajaj. Submitted for possible open access publication under the terms and conditions of the Creative Commons Attribution (CC BY) license (<http://creativecommons.org/licenses/by/4.0/>).